2021 EAGE ANNUAL
82ND CONFERENCE & EXHIBITION
AMSTERDAM | THE NETHERLANDS

MITIGATING CYCLE SKIPPING IN FULL-WAVEFORM INVERSION USING PARTIAL MATCHING FILTERS

J. Cooper[1], A. Ratcliffe[1], G. Poole[1]

[1] CGG

Summary

Existing methods for addressing cycle skipping in full-waveform inversion (FWI) typically involve either a modification of one of the data sets used to compute the least-squares objective function, or a reformulation of the objective function itself, often in terms of a traveltime (or equivalent) misfit. Both approaches can be successful, but they are reliant to varying extents on the notion of event similarity – that is, the requirement that the observed and modeled data contain the same, distinct, seismic events, even if the corresponding kinematics are different. We introduce a new technique for mitigating cycle skipping in FWI based on partial matching filters. The method accommodates amplitude differences between observed and modeled data, and does not require any major modification to an existing inversion engine. The proposed approach is validated on synthetic and real data sets, including an example where we observe a reduced reliance on event similarity compared to an established cycle skipping mitigation technique.

Introduction

Cycle skipping is a well-known problem in full-waveform inversion (FWI). It occurs when the timing of the modeled waveform (predicted by the current velocity model) differs from that of the observed waveform (obtained from recorded seismic data) by more than half a cycle. In this situation the conventional, least-squares, gradient-based FWI objective function converges to a local minimum and an erroneous velocity model. For a variety of reasons (for example, geological complexity or a lack of well log information), it can be difficult to derive a sufficiently accurate starting model to avoid cycle skipping at a given frequency. Starting the inversion at a lower frequency can reduce the likelihood of cycle skipping, but may not be viable as it depends on the quality of the acquired low frequency data.

Methodologies have been proposed to mitigate cycle skipping by using alternative objective functions (for example, Luo and Sava, 2011; Warner and Guasch, 2014; Métivier et al., 2016; Messud and Sedova, 2019). The use of objective functions based on traveltime differences between observed and modeled data can avoid cycle skipping (Luo and Schuster, 1991; Luo and Hale, 2013; Jiao et al., 2015; Zhang et al., 2018). However, this requires reliable estimation of these time differences (which can be challenging) and depends on event similarity (the same, distinct events being present in both data sets, albeit with different kinematics). Another strategy is to retain the conventional form of the objective function, and avoid cycle skipping by modifying one of the data sets used to compute the residual. For example, registration-guided least-squares inversion (Baek et al., 2014) and dynamic-warping FWI (Wang et al., 2016) replace the observed data at each iteration with an auxiliary data set, obtained by warping one data set partially towards the other using dynamic time shifts, such that they are not cycle skipped. These methodologies can be effective, but again rely on event similarity and accurate estimations of time shifts. Alternatively, Li and Demanet (2016) artificially extend the usable bandwidth of the observed data, thus avoiding cycle skipping by enabling FWI to start at a lower frequency. However, accurate extrapolation of low frequency data is a significant challenge.

Here we introduce an approach for mitigating cycle skipping using partial matching filters (PM-FWI). The method is compatible with conventional FWI frameworks, accommodates amplitude differences between observed and modeled data, and can alleviate reliance on event similarity.

Methodology

Consider two sets of N common shot gathers, d_n and u_n ($n = 1, \dots, N$), respectively representing the observed data and the corresponding forward modeled data based on the velocity model, $\boldsymbol{m}$. The conventional, least-squares FWI objective function, $\mathrm{J}(\boldsymbol{m}; d_n, u_n)$, is given by

$$\mathrm{J}(\boldsymbol{m}; d_n, u_n) = \sum_n \sum_k \sum_i (d_n[k,i] - u_n[k,i])^2 \ , \qquad (1)$$

where k and i index the receivers and time samples, respectively, in each shot gather, and we assume that any required preconditioning of the data is implicit in the definitions of d_n and u_n.

If $\boldsymbol{m}$ is sufficiently inaccurate to cause cycle skipping, we propose to replace the observed data d_n in Equation (1) with auxiliary data, p_n, obtained by considering matching filters connecting d_n to u_n, and applying them to d_n. Each iteration of FWI then proceeds as usual, but using the objective function $\mathrm{J}(\boldsymbol{m}; p_n, u_n)$. Auxiliary data generated with matching filters can describe differences between observed and modeled data with more flexibility than the dynamic time shifts discussed above.

While the matching filters are constructed to avoid cycle skipping between p_n and u_n, a key aspect of our approach is that they are designed specifically *not* to achieve a complete match of the observed data to the modeled data, as this would result in no meaningful FWI update. Instead, we seek a *partial* match: that is, we require that p_n is intermediate between d_n and u_n in such a way that the gradient obtained from $\mathrm{J}(\boldsymbol{m}; p_n, u_n)$ perturbs the velocity model in the same direction as the true perturbation.

Conventional 1D matching filters can be derived by minimizing $\sum(a - b * f)^2$, where a filter, f, is found to optimally approximate a data set, a, via convolution with a second data set, b, the summation carried out over all data points in a and b. This can be extended to higher dimensional cases as required. Verschuur (2006) recalls that the optimal least-squares Wiener filter is obtained by solving

$$\Phi_{a,b} = \Phi_{b,b} f \ , \qquad (2)$$

where $\Phi_{b,b}$ is the autocorrelation matrix of b, and $\Phi_{a,b}$ is the cross-correlation vector of a and b.

We seek a partial matching filter, not achieving a complete match of b to a, but sufficient to avoid cycle skipping. This may be obtained either by constraining the derivation of f in Equation (2) (for example, with appropriate sparseness weights) or by post-processing a conventional matching filter (for example, application of an external scaling operator to a conventional filter, f, designed to limit the extent to which the post-processed filter can modify the data). We adopt the latter approach here.

Results

Our first example is a 2D synthetic data set supplied by Chevron which formed the basis of an industry-wide FWI benchmark for an SEG workshop in 2014. It comprises 1,600, marine, flat-tow, isotropic, elastic, synthetic shot records with a record length of 8 seconds, a maximum offset of 8 km and limited signal below 3.5 Hz. We believe the geology of this example is based on field data from offshore Western Australia. Diving wave penetration is limited to ~1.8 km, corresponding to the maximum depth shown in Figure 1. The starting V_P velocity model for all tests is shown in Figure 1a and we perform acoustic, time-domain FWI. Figure 1f shows a pre-existing (~45 Hz) model which is known to be very accurate (the true model has yet to be released by Chevron, so is not available for direct comparison). Figure 1b shows the conventional FWI result at 5 Hz, exhibiting the effects of severe cycle skipping. Figure 1c shows application of FWI at 5 Hz using an approach outlined in the introduction, designed to mitigate cycle skipping by replacing the observed data at each iteration with a partially warped, auxiliary data set. This resolves the cycle skipping issue on the right hand side of the model (inside the black box), but not on the left hand side (inside the red box). Figures 1d and 1e show applications of PM-FWI: cycle skipping is avoided at 5 Hz (1d), and the subsequent application up to 20 Hz (1e) agrees well with the pre-existing result shown in Figure 1f.

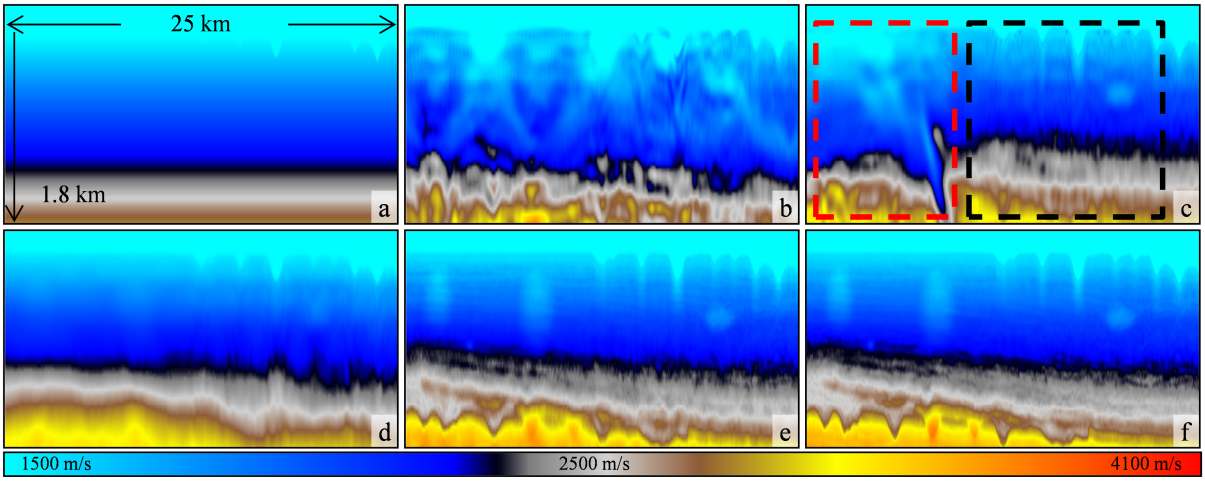

Figure 1 *PM-FWI on 2D synthetic data: (a) starting model, (b) conventional FWI at 5 Hz, (c) FWI at 5 Hz using partially warped data, (d) PM-FWI at 5 Hz, (e) PM-FWI up to 20 Hz, and (f) a pre-existing, very accurate model.*

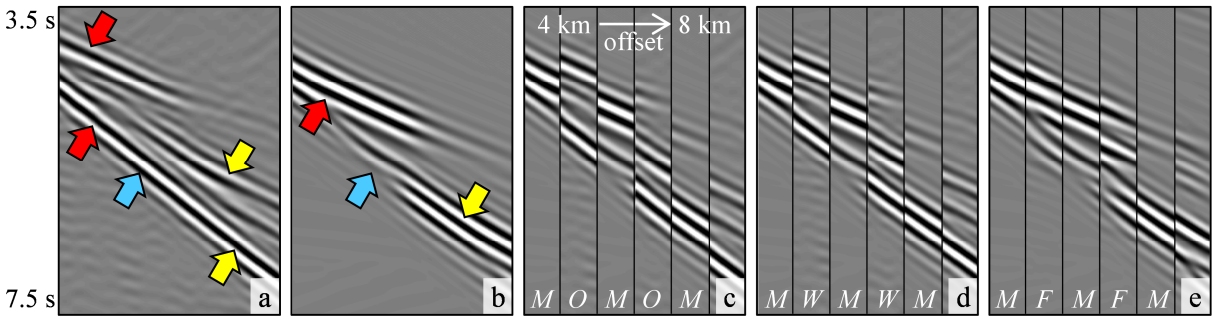

Figure 2 *(a) Observed, and (b) modeled shots in a region without event similarity; modeled data, M, interleaved with (c) observed data, O, (d) partially warped data, W, and (e) partially matched data, F.*

Figures 2a and 2b respectively show observed and modeled data (using the model in Figure 1a), from a shot gather in the region where FWI using partially warped data fails to address the cycle skipping

issue. Comparison of these two figures identifies three key features, each of which can be interpreted as a lack of event similarity. The red and yellow arrows both highlight regions where two distinct events in the observed data overlap in the modeled data, such that only one event is evident. Further, the interference caused by this overlap results in an apparent difference in the structure of an event, highlighted by the blue arrow. These differences are further emphasized in Figure 2c, in which the observed and modeled data are interleaved. Figures 2d and 2e show a corresponding interleaving of partially warped data with modeled data, and partially matched data with modeled data, respectively. These figures demonstrate that the increased flexibility of the partial matching filters allows for the lack of event similarity to be handled more effectively than in the case of the partial warping. We believe all cycle skipping mitigation methods reliant on event similarity would experience difficulties here. The partial warping result might be improved by starting the inversion at a lower frequency, by careful re-parameterization of the warping parameters, or by a surgical mute in the preconditioning for the inversion, none of which was necessary for the PM-FWI result shown here.

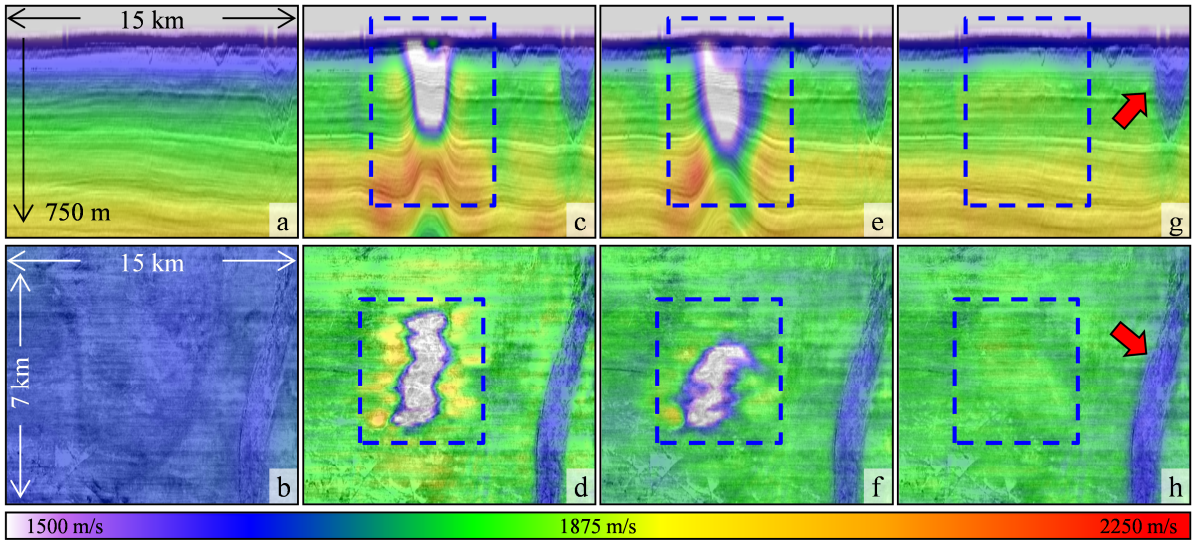

Figure 3 *PM-FWI on 3D field data: (a) and (b) starting model, (c) and (d) FWI at 5 Hz, (e) and (f) FWI at 4 Hz, (g) and (h) PM-FWI + FWI at 5 Hz.*

Our second example is taken from a real, 3D, towed streamer data set from the Norwegian North Sea. Figure 3 shows V_P velocity models overlaid on corresponding Kirchhoff depth migration stacks: the top half of the figure shows an inline section, the bottom half shows a depth slice at 240 m through the shallow anomalies. Figures 3a and 3b show the starting model. FWI is applied at 5 Hz (Figures 3c and 3d) revealing a localized cycle skipping issue (highlighted by the blue boxes) – Figures 3e and 3f show this is not overcome by instead applying FWI at the lower starting frequency of 4 Hz. Figures 3g and 3h show PM-FWI at 5 Hz followed by conventional FWI at 5 Hz. This avoids cycle skipping while still identifying the real shallow channel feature (highlighted by the red arrows), and will allow conventional FWI to proceed to higher frequencies in the usual manner. Figure 4 shows the depth migrations in more detail, the red arrows indicating improved stack response and structural conformity after PM-FWI followed by conventional FWI (Figure 4b) compared to the starting model (4a).

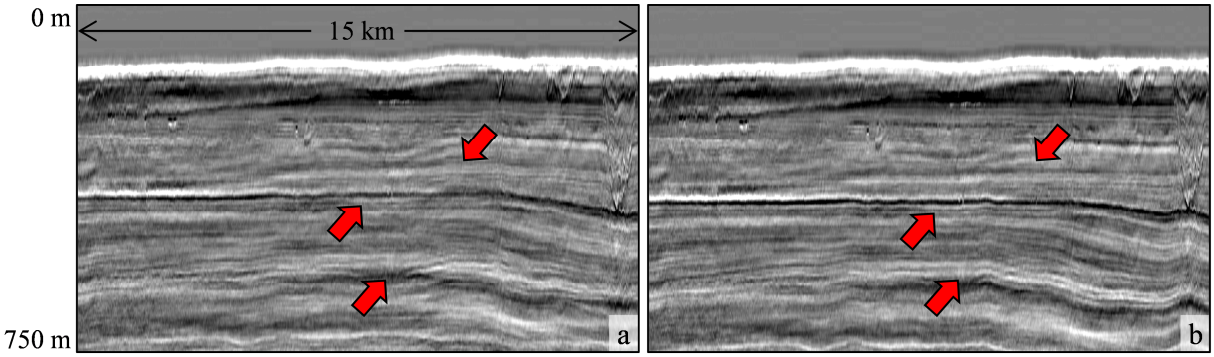

Figure 4 *PM-FWI on 3D field data: Kirchhoff depth migrations using: (a) starting model, and (b) model after PM-FWI + FWI at 5 Hz.*

Discussion

PM-FWI is straightforward to implement by inserting the partial matching operation into a conventional, least-squares FWI engine – no other modification of the objective function or inversion scheme is needed. It is flexible enough to be used as the FWI result itself, or as a preconditioner for a subsequent application of least-squares or other forms of FWI. However, our approach is not immune to extreme discrepancies between observed and modeled data. Specifically, for partial matching filters to operate appropriately we require some meaningful content in both data sets. Also, if traveltime differences between the observed and modeled waveforms exceed the matching filter length, then the method will fail and testing will be required to obtain a good result. PM-FWI may also converge more slowly than conventional FWI, as the step length at each iteration seeks to minimize the misfit of the partially matched data and the modeled data, which can be small even for an inaccurate model. The convergence may be accelerated by, for example, an appropriate over-relaxation of the step length.

Finally, we highlight that, while PM-FWI can be incorporated into velocity and anisotropy diving-wave-only FWI to alleviate cycle skipping, it does not resolve the underlying multi-parameter cross-talk inherent in these schemes. Also, if the real world (visco-elastic) behavior causes the overall phase response from the different interacting waveforms to change compared to our acoustic implementation, PM-FWI will still suffer from the physics missing in our velocity model.

Conclusions

We propose a new approach for mitigating cycle skipping in FWI using partial matching filters. It accommodates amplitude differences between observed and modeled data and uses the conventional form of the objective function. We have demonstrated PM-FWI's effectiveness on synthetic and field data, including an example where we find a reduced reliance on event similarity relative to a partial warping approach. The method is also suitable as a preconditioner for other formulations of FWI.

Acknowledgements

We thank CGG for permission to publish and CGG Multi-Client & New Ventures for permission to show the field data example. We also thank Chevron for providing the 2D synthetic data set.

References

Baek, H., Calandra, H. and Demanet, L. [2014] Velocity estimation via registration-guided least-squares inversion. *Geophysics*, **79**(2), R79–R89.

Jiao, K., Sun, D., Cheng, X. and Vigh, D. [2015] Matching pursuit full waveform inversion. *77th EAGE Conference and Exhibition*, Extended Abstracts, We N104 08.

Li, Y. E. and Demanet, L. [2016] Full-waveform inversion with extrapolated low-frequency data. *Geophysics*, **81**(6), R339–R348.

Luo, S. and Hale, D. [2013] Separating traveltimes and amplitudes in waveform inversion. *83rd Annual International Meeting, SEG*, Expanded Abstracts, 969-974.

Luo, S. and Sava, P. [2011] A deconvolution-based objective function for wave-equation inversion. *81st Annual International Meeting, SEG*, Expanded Abstracts, 2788-2792.

Luo, Y. and Schuster, G. T. [1991] Wave-equation traveltime inversion. *Geophysics*, **56**(5), 645-653.

Messud, J. and Sedova, A. [2019] Multidimensional optimal transport for 3D FWI: demonstration on field data. *81st EAGE Conference and Exhibition*, Extended Abstracts, Tu R08 02.

Métivier, L., Brossier, R., Mérigot, Q., Oudet, E. and Virieux, J. [2016] Measuring the misfit between seismograms using an optimal transport distance: application to full waveform inversion. *Geophysical Journal International*, **205**(1), 345-377.

Verschuur, D. J. [2006] Seismic multiple removal techniques: past, present and future. EAGE publications.

Wang, M., Xie, Y., Xu, W. Q., Xin, K. F., Chuah, B. L., Loh, F. C., Manning, T. and Wolfarth, S. [2016] Dynamic-warping full-waveform inversion to overcome cycle skipping. *86th Annual International Meeting, SEG*, Expanded Abstracts, 1273-1277.

Warner, M. and Guasch, L. [2014] Adaptive Waveform Inversion – FWI without cycle skipping – theory. *76th EAGE Conference and Exhibition*, Extended Abstracts, We E106 13.

Zhang, Z., Mei, J., Lin, F., Huang, R. and Wang, P. [2018] Correcting for salt misinterpretation with full-waveform inversion. *88thAnnual International Meeting, SEG*, Expanded Abstracts, 1143-1147.